Incorporating multi-region crack growth into mechanical reliability predictions for optical fibres

T. A. HANSON, G. S. GLAESEMANN
Corning Incorporated, Corning, NY 14831, USA

Most mechanical reliability models for optical fibre assume the same crack growth parameters (n and B) for both proof testing and in-service life. However, this assumption leads to inconsistencies in our understanding of how the fibre behaves in the laboratory and in the field. In 1983 Ritter et al. suggested that proof-testing and in-service crack growth parameters differ according to their respective environments. Recent high-speed strength tests of abraded optical fibres indicate that crack-growth parameters change as a function of time under the same environmental conditions. It was suggested that at high processing speeds, the presence of crack growth in Region II of the K-V relationship should be entertained. In this work, the impact of Region II crack growth during proof testing was explored and the effect on mechanical reliability predictions evaluated.

1. Introduction

The power law has long been used as a model of flaw growth and as a basis of computing the reliability of fused silica-clad optical fibre. Most fibres are proof tested at a nominal proof stress of 0.69 GPa (10^5 p.s.i.) during manufacturing to remove large flaws from the population. This paper will demonstrate that the standard Region I power law is insufficient for completing the analysis of the reliability of proof-tested fibre and that incorporating the effect of Region II should be considered.

Fuller *et al*. [1] showed that, with the single-region power law, the minimum surviving strength depends on the proof stress and unloading time in a relationship with the stress corrosion parameter, *n*, and the *B* parameter according to a complex arrangement. The relationship depends on whether unloading is "fast", or "slow". "Fast" corresponds to conditions in which unloading is sufficiently fast for no unloading failures to occur. In "slow" unloading, the minimum surviving strength is only a function of the unloading rate, and can approach zero as *B* approaches zero. Hence the value of *B* has direct relevance to the reliability derived from conducting a proof test for both "fast" and "slow" conditions.

Various values of *B* have been reported in the literature (from 5×10^{-9} to 0.5 GPa²s). Glaesemann and Helfinstine [2] conducted inert testing on weak fibres and concluded that *B* is around 5.8×10^{-4} GPa²s by comparing strength measured at -120°C to room-temperature dynamic fatigue measurements at 4% min⁻¹. This low value of *B* would suggest that most proof-test unloading rates may not be fast enough to preclude proof-test unloading failures.

Consequently, the minimum surviving strength could be significantly less than the proof stress.

This result is not consistent with historical field data. Tens of millions of kilometres of fibre have been installed with bend stress ranging from 20%-30% of the proof stress. At most, only a handful of fatigue-related failures have been reported.

The following dynamic fatigue experiment was conducted to explore the phenomena of high-speed fracture in more detail. Note that these results were previously published [3], but it is useful to review the results here. These results have led the authors to conclude the Region II, as described by Lawn [4], plays an important role in high speed events such as proof testing dynamics.

2. Experimental procedure

Fibre testing with commonly used universal tensile machines allows for maximum strain rates in the 100% min⁻¹ range. To achieve higher strain rates for this study, a belt slide system was employed [3]. This apparatus is shown schematically in Fig. 1. Fibres are attached to a piezoelectric load cell mounted on a rigid station at one end and a capstan mounted on a belt slide system at the other end. The belt slide is driven by a stepper motor and is capable of a maximum strain rate of approximately 5000% min⁻¹, or a stressing rate of 57GPas⁻¹. A small amount of slack in the gauge length of the fibre allows the belt slide to reach maximum velocity before the fibre experiences appreciable tension. Load versus time data are taken using a digital oscilloscope. All tests were performed in a laboratory ambient environment that was 40%-50% RH and 23 °C.

The slowest strain rate provided by this belt slide system is 30% min⁻¹, and therefore, a conventional screw-driven tensile testing method was used to provide strength data at slower strain rates. Nominal strain rates from 0.0025% min⁻¹ to 25% min⁻¹ were used.

The silica-clad fibre used in this study was manufactured in a conventional manner with the exception that it was intentionally abraded during the draw process to a strength near typical proof-stress levels. The abrasion technique consisted of lightly pressing a 150 μm glass fibre against the fibre being drawn prior to application of the polymer coating. All the data for the twelve rate are shown in Fig. 2 in Weibull fashion.

The logarithm of the median failure stress for each nominal rate, plotted versus the logarithm of stress rate is shown in Fig. 3. The fitted line relates to the value of n (24.5) that would be measured using the lower rates, which correspond to those used in TIA Fibre Optic Test Procedure-76 [5].

The failure stresses at the higher rates form a reverse pattern from that expected from the power law, which predicts either a linear extension of the line in Fig. 3, or a flattening out of the curve at the higher rates once the pre-fatigue strength had been reached. The increase in the slope at higher rates suggests a lower n for high stress rates and that Region II of the K-V curve may be the cause. Region II would thus play an important role in determining the strength degradation in fast stress rate events such as proof-test unloading.
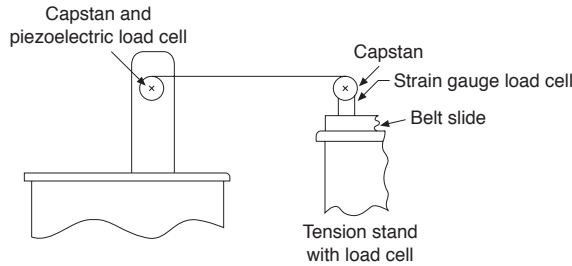
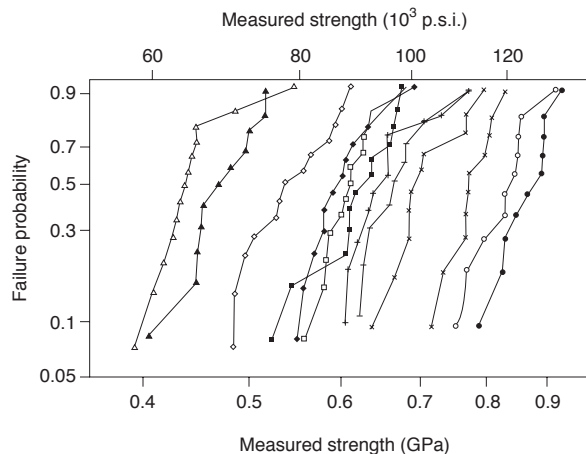*Figure 1* Schematic drawing of the belt slide tensile testing apparatus.

Figure 2 Experimental results of high-speed testing plotted in Weibull fashion.
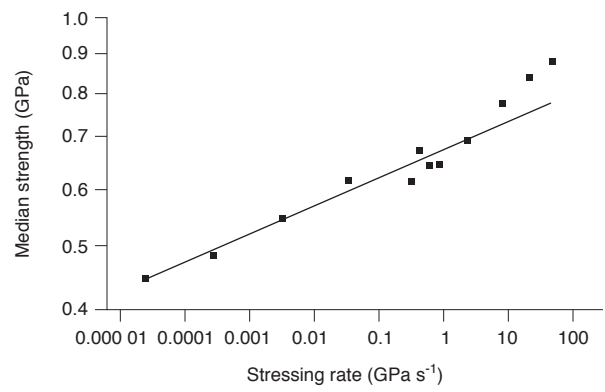
Figure 3 Stress and stress rate plotted for median strength values.

3. Two-region power-law mathematics

It is well known that subcritical crack growth in many glasses follows the classic schematic curve in Fig. 4 where crack velocity, da/dt, is plotted as a function of the stress intensity factor, K_I. Three regions of crack growth have been identified and thoroughly discussed in the literature [4]. In this work, we are primarily concerned with incorporating the effects of Region II type crack growth into conventional models for subcritical crack growth in Region I. To do this, we model these regions as two power laws, each having different slopes which we will call n_1 for the usual Region I, and n_2, describing Region II. This is shown schematically in Fig. 5. There are corresponding B_1 and B_2 values as well. The two-region power law can be written as

$$\frac{da}{dt} = \upsilon \left(\frac{K_I}{K_{Ic}} \right)^{n_2} \qquad \text{for } K_I \geq \qquad (1)$$

$$\frac{da}{dt} = \upsilon r^{n_2-n_1} \left(\frac{K_I}{K_{Ic}} \right)^{n_1} \qquad \text{for } K_I \leq rK_{Ic} \qquad (2)$$

where K_I is the mode I stress intensity factor, K_{Ic} is the critical stress intensity factor associated with failure, da/dt is the flaw growth rate, υ is the critical velocity, and rK_{Ic} is the K_I value in the K-V curve where Regions I and II intersect.

Equations 1 can be rewritten in terms of the changing strength, S, and applied stress, σ, using conventional fracture mechanics, $K_I = Y\sigma a^{1/2}$ and $K_{Ic} = YSa^{1/2}$. For dynamic fatigue at constant stressing rate to failure, the following equations govern the relation between strength and failure stress for Regions I and II growth, respectively

$$S_0^{n_1-2} = S_r^{n_1-2} + \frac{\sigma_r^{n_1+1}}{B_1(n_1+1)\dot\sigma} \qquad (3a)$$

$$S_r^{n_2-2} = \sigma_f^{n_2-2} + \frac{\sigma_f^{n_2+1} - \sigma_r^{n_2+1}}{B_2(n_2+1)\dot\sigma} \qquad (3b)$$

where S_0 is the strength before loading, S_r and σ_r are the strength and stress when $\sigma_r/S_r = r$, σ_f is the failure stress, $\dot\sigma$ is the stress rate, $1/B_2 = \upsilon(n_2-2)/ 2 (Y/K_c)^2$, and $B_1 = B_2 r^{n_1-n_2} (n_1-2)/(n_2-2)$.

A physical description of failure for the two region model in Equation 3 would be that while loading under a constant stress rate, a flaw with initial strength, S_0, experiences typical Region I growth as
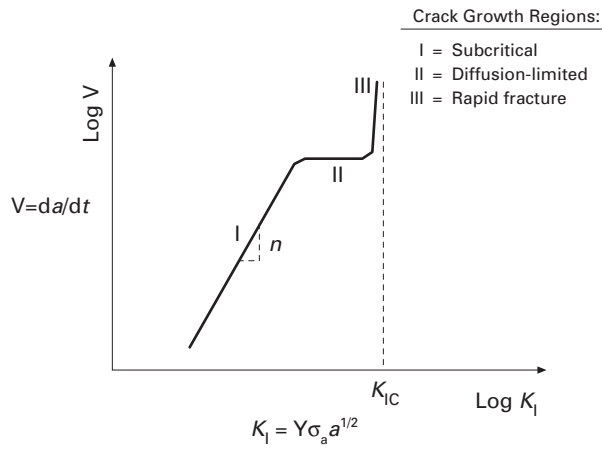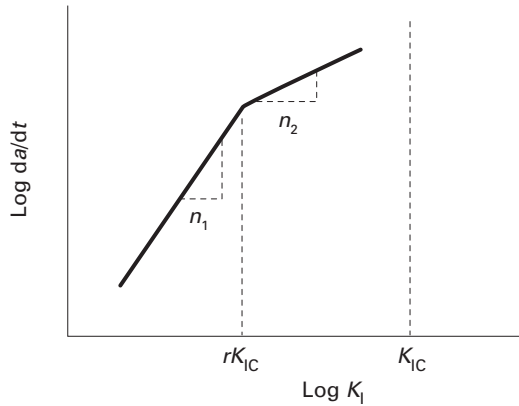
Figure 4 Class K-V curve for silica glass.

Figure 5 Schematic drawing of the two-region power-law model.

expressed by Equation 3a and degrades to strength, S_r. At strength, S_r, the growth behaviour transitions to that of Region II and the flaw degrades to the final strength, σ_f. Note that when the flaw has grown to strength S_r, the applied stress is σ_r.

To determine the initial strength from a failure stress, one must iteratively solve for σ_r and S_r using Equation 3b, then calculate S_0 using Equation 3a. To compute the failure stress for a given initial strength, the reverse process is performed.

The above analysis was performed for the case of dynamic fatigue. A more general treatment of crack-growth mechanics of Regions I and II, respectively, is expressed as

$$S(t_{min})^{n_1-2} = S(t_{max})^{n_1-2} + \frac{1}{B_1} \int_{t_{min}}^{t_{max}} \sigma(t)^{n_1} dt$$

$$\text{for } t \text{ such that } \frac{\sigma(t)}{S(t)} < r \quad (4a)$$

$$S(t_{min})^{n_2-2} = S(t_{max})^{n_2-2} + \frac{1}{B_2} \int_{t_{min}}^{t_{max}} \sigma(t)^{n_2} dt$$

$$\text{for } t \text{ such that } \frac{\sigma(t)}{S(t)} > r \quad (4b)$$

In this manner, a flaw passes through Region II on the way to failure. Using failure stress and any stress history, one can solve for the various possible cross-

ings between Regions I and II. This will be done for the proof test in a following section.

4. Two-region power law applied to experimental data

A fundamental assumption of all fatigue parameter evaluation algorithms is that the initial strength distribution for each stress rate is drawn from the same statistical population of flaws. Central statistics, such as median or average, of the computed initial strength should therefore be the same for each rate. The fatigue parameter values for which the agreement is best are taken to be the best estimates of the fatigue parameter values.

Equations 3a and b were used to compute the initial strength of the middle three failure stress values for each stress rate for the data in Fig. 2. This was done for many combinations of n_1, n_2, B_2, and r, in a four-dimensional binary search. Fig. 6 shows the measured failure stress values from Fig. 3 and the computed initial strength for the best parameter values. A summary of computed crack-growth parameters is given in Table I.

The fact that the computed initial strength results in Fig. 6 are the same for all stressing rates indicates that the model appropriately incorporated the non-linear behaviour of the dynamic fatigue data. It also gives one confidence in drawing conclusions about the true initial strength of flaws in fibres, a required value for accurate reliability predictions.

Fig. 6 shows that for normal rates, the ratio of failure stress to strength is 0.6, which corresponds to low values of B in the context of the standard power law. For higher rates, the ratio of failure stress to initial strength rapidly approaches 1, which corresponds to a high value of B using the standard power
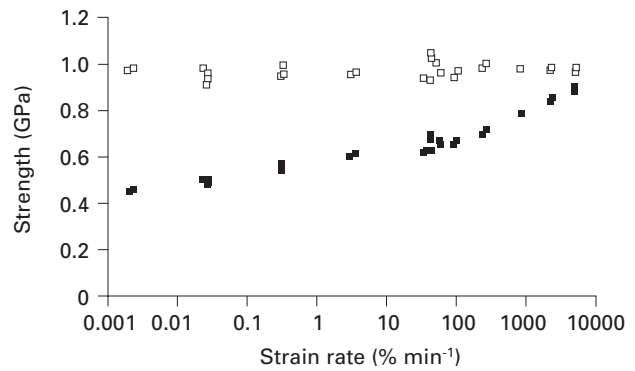

Figure 6 (■) Measured failure stress data and (□) computed initial strength.

TABLE I. Fitted fatigue parameters for the two-region power-law model

n_1	21
n_2	4.5
r	0.645
B_1	4.5×10^{-5} GPa^{2}s
B_2	0.0082 GPA^{2}s

law. In effect, there are two B values. The one that is dominant depends on the stressing rate. The factor of 0.6 is in general agreement with low temperature measurements of Proctor *et al.* [6] and Glaesemann and Helfinstine [2].

The n value in Table I for Region I is within the range of accepted values. The B value for Region I, B_1, is within the range of values predicted from low-temperature testing of abraded optical fibres [2]. Using a value of 0.75 MPa m$^{1/2}$ for K_{Ic}/Y, the value of B_2 leads to a computed critical velocity, v, of 0.055 mm s^{-1}. If one were to ignore Region II, as is usually done, the critical velocity from Region I data is determined to be 1.3 mm s^{-1}.

The predicted transition from Region I to Region II crack growth from the high-speed fibre strength data, rK_{Ic}, is 65% K_{Ic}. This predicted transition from Region I to II is less than the value of 80% K_{Ic} reported by Weiderhorn on bulk fused silica [7]. There are a number of factors that could explain this difference, such as the difference in Region I crack growth between silica fibre and bulk silica or an influence of the optical fibre coating. This remains as an interesting area of further research.

This analysis of high-speed strength data using a two-region crack growth model can be used to model strength degradation for a more complex stress history, namely that of proof testing.

5. Implications
5.1. Proof testing
The effect of Region I crack growth has been thoroughly discussed in previous publications [1, 8], and therefore, a level of familiarity is assumed. Fig. 7 below illustrates the basic proof test event. Fibre is loaded at a stressing rate, $\dot{\sigma}$, to a predetermined proof stress level, σ_p, held for some period of time, t_d, and subsequently unloaded at rate $\dot{\sigma}_u$. This is shown as the solid line in the illustration.

We have chosen to examine the effect of proof testing on the flaw that just survives the event. This is done for two reasons, first, the modelling of this flaw has been the source of extensive effort and interest and, second, this flaw is the weakest one to be placed in service. Extending the two-region power-law model to a distribution of flaws can be done and will be published at a later time.

The flaw that just passes proof testing begins with a pre-proof test strength labelled S_{1min} in Fig. 7. It degrades during proof testing to a strength level, S_{pmin}, by the time the dwell time is over. Now, as the stress is removed during unloading, the flaw has the opportunity to continue growing as stress still exists. It does so until it just survives an applied stress which is equal to the strength of a flaw that just fails, σ_{fmin}. After just surviving, it grows to a final strength S_{2min}. The final strength, S_{2min}, can be less than the proof stress, σ_p, if the unloading time is slow enough. In other words, what happens during unloading is the key to the final strength. This is where we make a closer examination of the proof-test event using the two-region power-law model.
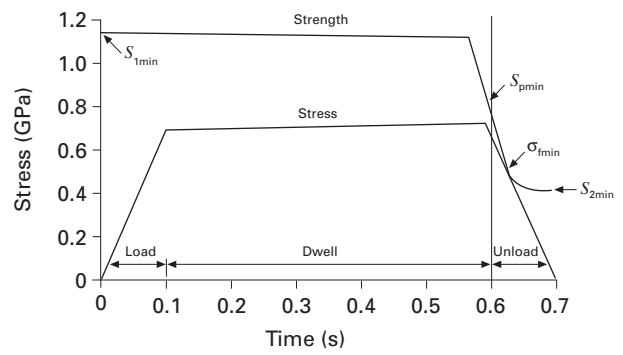

Figure 7 Schematic drawing of a typical proof test event.

The basic methodology for modelling the unloading event is as follows. The minimum surviving strength, S_{2min}, is determined from (1) the minimum strength at the start of unloading, S_{pmin}, that just fails at σ_{fmin}, (2) the proof stress, σ_p, and (3) the unloading time, t_u, assuming a linear stress reduction with time [1]. To determine S_{2min}, S_{pmin} is determined first and then reduced through fatigue to S_{2min}, during the unloading process. A flaw that "just fails" is defined by a flaw-growth curve such that the stress intensity ratio, K_I/K_{Ic}, has a maximum at the value of 1. There are two cases involving Region II growth at the start of unloading. The outcome is governed [1] by the parameter, α

$$\alpha = \frac{\sigma_p^3}{B_2(n_2 - 2)\dot{\sigma}_u} \tag{5}$$

where $\dot{\sigma}_u = \sigma_p/t_u$ and the crack-growth parameters come from Region II. The values of S_{pmin} and S_{2min} are determined with different equations, depending on whether $\alpha \leq 1$ or $\alpha > 1$.

Case 1: $\alpha \leq 1$. This is where the unloading time is sufficiently fast that K_I/K_{Ic} decreases throughout the unloading time. This is shown schematically as "fast unload" in Fig. 8 where the ratio K_I/K_{Ic} is plotted versus unload time. In this case, K_I never reaches K_{Ic} and K_I/K_{Ic} has a negative slope throughout. Therefore, no fatigue to failure can occur during unloading in this case and the strength of a flaw that just fails, σ_{fmin}, is equal to the proof stress. The limit case for this behaviour for flaws near a proof stress level of 10^5 p.s.i. is $\alpha = 1$ and the unloading rate is determined to be 20 GPas^{-1} using the two-region power law.

Case 2: $\alpha > 1$. In this case the flaw begins unloading in the Region II growth range, but the unloading rate, while still fast, results in K_I/K_{Ic} initially increasing. This is shown as "slow unload" in Fig. 8 where the flaw that just survives is the one where the unloading rate is such that K_I/K_{Ic} tangentially approaches 1 and just nearly fails. In this case the strength of the flaw that just survives, S_{pmin}, at the beginning of unloading can be determined from

$$S_{pmin}^{n_2-2} = \frac{3}{n_2 + 1}\left[B_2(n_2 - 2)\dot{\sigma}_u\right]^{(n_2-2)/3}$$
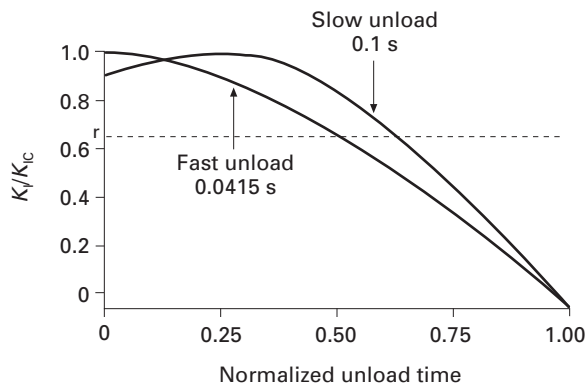$$+ \frac{\sigma_p^{n_2+1}}{B_2(n_2 + 1)\dot{\sigma}_u} \tag{6}$$

Figure 8 Dependence of the stress intensity factor on unload time for various unloading cases.

and the strength of the flaw that just fails during unloading is

$$\sigma_{fmin} = \left[B_2(n_2 - 2)\dot{\sigma}_u\right]^{1/3} \tag{7}$$

For both cases, the just surviving flaw continues to grow, and when K_I/K_{Ic} decreases to r, crack growth moves into Region I. Thus, in order to determine the final surviving strength, it is necessary to determine the strength, σ_r, at the transition between regions by iteratively solving

$$\sigma_r^{n_2-2}\left[\frac{1}{r^{n_2-2}} - \frac{\sigma_r^3}{B_2(n_2 + 1)\dot{\sigma}_u}\right]$$

$$= \sigma_{fmin}^{n_2-2}\left[1 - \frac{\sigma_{fmin}^3}{B_2(n_2 + 1)\dot{\sigma}_u}\right] \tag{8}$$

Using the computed value of σ_r, the minimum surviving strength is given by

$$S_{2min}^{n-2} = \left(\frac{\sigma_r}{r}\right)^{n-2} - \frac{\sigma_r^{n+1}}{B_1(n + 1)\dot{\sigma}_u} \tag{9}$$

One can also compute the initial, pre-pre-proof test strength, S_{1min}, that leads to the minimum surviving strength using a similar, but simpler process. Basically, it involves backing up through the proof-test event beginning at the end of the dwell time where S_{pmin} is known. Depending on the loading rate and dwell time, the flaw will initially have Region I growth and move into Region II growth either during loading or the dwell time. If the transition occurs during loading, the strength at the end of loading is determined using Region II equations followed by the application of the previously presented dynamic fatigue equations to determine the strength during loading where the flaw transitions from Region I to Region II. Well-known Region I crack-growth mechanics can then be used to determine the initial strength before loading.

If the transition occurs during the dwell time, the time at which the transition occurs is determined using Equation 4b after which Equation 4a yields the pre-proof strength.

From a practical point of view, it is useful to determine the unloading rate above which no strength degradation to failure can occur during unloading. As σ_{fmin} approaches the proof stress in Equation 7 one can determine the unloading rate where the model

transitions from $\alpha \le 1$ or $\alpha > 1$. Using the crack-growth parameters in Table I and a proof stress of 0.73 GPa, the unloading rate is determined to be 20 GPas^{-1}. If unloading is faster than 20 GPas^{-1}, it is predicted that there will be insufficient time for crack growth to failure during unloading.

Case 3: Region I type growth at the start of unload. This case applies primarily to those proof testing events that have a relatively slow unloading rate. If the computed value of σ_p/S_{pmin}, is less than r, this case applies. This unloading case might be found in situations such as the proof testing of splices and connectors. There are basically two scenarios for this case. One is where a flaw starts in Region I and transitions into Region II before the end of unloading. The second is where the unloading rate is slow enough that the flaw that just survives can never reach Region II type growth. The mathematics for this case is reviewed in the Appendix. The point here is that the complex scenarios brought on by considering multi-region crack growth can be successfully modelled.

5.2. Lifetime determinations for the flaw just passing the proof-test event

Once the post-proof-strength distribution has been established, the two-region power-law model can be used to model in-service life. Actually, because most crack growth over a 25 or 45 year life is Region I type growth, the Region II influence on such fibre lifetimes will be small.

For the purpose of this paper, we limit the lifetime prediction to that of the largest flaw, S_{2min}. The maximum static applied stress, σ_a, for a flaw with a post proof strength of S_{2min} to survive a service life, t_f, is, determined by computing the time for the onset of Region II using Equation 4a, followed by application of Equation 4b to determine the additional time to grow to failure in Region II. Table II shows the results of these calculations for an assumed set of proof-test conditions and the fatigue parameters from Table I.

T A B L E II. Minimum surviving strength and lifetime determinations

Proof stress (GPa)	0.73
(10^3 p.s.i.)	105
Dwell time (s)	0.3
Unload time (s)	0.01
Unload rate (GPa s^{-1})	73
$\alpha(\alpha<1)$[a]	0.26
S_{1min}, minimum initial strength to survive proofing (GPa)	1.17
(10^3 p.s.i.)	169
S_{pmin}, minimum strength at unload (GPa)	0.73
(10^3 p.s.i.)	105
S_{2min}, minimum surviving strength (GPa)	0.70
(10^3 p.s.i.)	100
Survival time (y)	25
Applied stress (GPa)	0.17
(10^3 p.s.i.)	25
Applied stress/(min. surviving strength, S_{2min})	0.25
Applied stress/proof stress	0.23

[a]For this example, the case of very fast unloading is used, $\alpha \le 1$, such conditions can be achieved on typical equipment for proof testing long lengths of fibre.

5309

Thus, this model predicts that a flaw just surviving case 1 unloading conditions will fail in 25 years if loaded to 23% of the proof stress. For a more conservative approach, where reliability is designed around 1% crack growth in 40 years, the allowable stress is determined to be 20% of the proof stress.

It is important to note that the above analysis used a proof stress of l05 x 10³ p.s.i which is the actual proof stress needed to satisfy FOTP-31C requirements for proofing at a nominal proof stress of 10⁵ p.s.i., for the given unloading time. That is to say, a slight over-proof testing is required under the FOTP. Using the nominal proof stress of 10⁵ p.s.i. the allowable stress for failure in 25 years simply becomes 25% of the nominal proof stress, and that for 1% crack growth in 40 years becomes 2l.5% of the nominal proof stress.

6. Conclusions

In recent years, it has become increasingly apparent that a single region of crack growth was insufficient to explain crack growth during both high-speed and long-term low-stress events. The incorporation of the well-known Region II into the crack growth model is helpful in explaining contradictions surrounding the B value as well as previously observed non-linear dynamic fatigue behaviour.

For high-speed events such as proof testing, Region II crack growth plays a significant role in establishing the post-proof strength distribution. This paper was confined to modelling the growth history of the weakest flaw. It was found that the incorporation of Region II crack growth generates several crack-growth scenarios and attempts were made at extending the model to each of them.

The case where a flaw just survived a high-speed proof test during manufacturing, was extended to in-service life. It was found that for 25 year life, an applied stress of 23% of the actual proof stress, or 25% of the nominal proof stress, is needed. A more conservative approach of allowing only 1% crack growth in 40 years results in an allowable applied stress of 20% of the actual proof stress, or 21.5% of the nominal proof stress.

Future work will examine the influence of multi-region crack growth on a distribution of flaw sizes. It is believed that this will provide a more accurate prediction of post-proof strength distributions needed in reliability predictions. In addition, experimental evidence is needed to support the modelling of slower speed proof-test events.

Appendix. Case 3: Region I type growth at the start of unload

There are two scenarios here. Scenario 1 is where the stress intensity factor starts at Region I and continues on into Region II. This is similar to Case 2 above, with the exception that the flaw begins in Region I. It is useful to consider this unloading scenario in two process steps. There is Region I growth to "r" followed by Region II growth. Again there is a flaw that just fails

or just survives and becomes the minimum strength flaw. Equation 7 gives the minimum failure stress, σ_{fmin}, for the flaw that just fails. Using this value, the following equation is iteratively solved to determine the stress, σ_{rp}, above σ_{fmin}, at which Region II must have started,

$$\sigma_{rp}^{n_2-2}\left[\left(\frac{1}{r}\right)^{n_2-2} - \frac{\sigma_{rp}^3}{B_2(n_2+1)\dot{\sigma}_u}\right]$$

$$= \sigma_{\text{fmin}}^{n_2-2}\left[1 - \frac{\sigma_{\text{fmin}}^3}{B_2(n_2+1)\dot{\sigma}_u}\right] \qquad (A1)$$

where σ_{rp} is the applied stress when $K_I/K_{Ic} = r$. Knowing, σ_{rp}, one can backup through the Region I growth portion of unloading process to determine the strength at the beginning of unloading. Note that Scenario 1 for this case is verified if K_I/K_{Ic} is increasing when condition r is reached using

$$\left(\frac{1}{r}\right)^{n_1-2} < \frac{\sigma_{rp}^3}{B_1(n_1-1)\dot{\sigma}_u} \qquad (A2)$$

The strength at the beginning of the unloading time, S_{pmin}, for this scenario is determined from

$$S_{\text{pmin}}^{n_1-2} = \left(\frac{\sigma_{rp}}{r}\right)^{n_1-2} + \frac{1}{B_1(n_1+1)\dot{\sigma}_u}(\sigma_p^{n_1+1} - \sigma_{rp}^{n_1+1}) \qquad (A3)$$

The minimum post-proof strength, $S_{2\text{min}}$, is computed from σ_{fmin} as previously described for the Region II case in Equations 8 and 9. The initial pre-proof strength that just passes proof testing, $S_{1\text{min}}$, is calculated using Equation 4a because only Region I growth occurs up to the start of unloading.

Scenario 2 is used when the inequality in Equation A2 is not true. Physically, this corresponds to the situation where a flaw that starts in Region I at the onset of unloading with K_I/K_{Ic} increasing with time, approaches r. However, in this case the unloading rate is such that if Region II growth occurs, the resulting K_I/K_{Ic} ratio immediately goes to 1 and the flaw fails. In other words, the flaw that just survives unloading experiences only Region I growth. Thus, the largest flaw that can just survive is one that has a K_I/K_{Ic} equal to r and a strength at the beginning of unload of the strength σ_p/r.

If K_I/K_{Ic} is decreasing at the beginning of unloading we have the situation where Region II is just avoided at the beginning of unloading. The following is true for this situation

$$\left(\frac{1}{r}\right)^{n_1-2} > \frac{\sigma_p^3}{B_1(n_1-2)\dot{\sigma}_u} \qquad (A4)$$

The minimum strength at the beginning of unloading, S_{pmin}, that survives unloading for this scenario is simply σ_p/r. Any flaw weaker than σ_p/r will transition into Region II during unloading and immediately fail.

Even more interesting is where growth is in Region I and K_I/K_{Ic} initially increases at the start of unloading. This occurs when the inequality in Equation A4 is not true. Here a flaw that is initially in Region I approaches Region II some time during unloading. If

the flaw is too weak it will enter into Region II and not survive unloading. The task is to find the maximum strength flaw that just avoids Region II. Of all the flaws that have just survived the proof stress over the dwell time, with general strength at that point called S_p, there is flaw with strength S_{pmax} at the beginning of unloading that degrades under Region I growth to a point where K_I/K_{Ic} just approaches r. The stress at this point is identified as σ_{max} and the strength of the flaw at σ_{max} is given as S_{max}.

The inequality in Equation A4 for this situation is not true and is rewritten as

$$\frac{\sigma_p}{S_p} < r \qquad \text{(A5a)}$$

and

$$\left(\frac{S_p}{\sigma_p}\right)^{n_1-2} < \frac{\sigma_p^3}{B_1(n_1-2)\dot{\sigma}_u} \qquad \text{(A5b)}$$

The condition in Equations A5a and b implies that Region I growth is occurring at the start of unloading and that the stress intensity ratio is increasing with time.

The stress, σ_{max}, at which the stress intensity ratio is maximum, is determined by setting the first derivative of the stress intensity ratio to zero to yield

$$\sigma_{pmax}^{n_1+1} = \frac{n_1+1}{3} B_1(n_1-2)\dot{\sigma}_u\left[S_p^{n_1-2} - \frac{\sigma_p^{n_1+1}}{B_1(n_1+1)\dot{\sigma}_u}\right] \quad \text{(A6)}$$

The strength, S_{max}, at which the maximum stress intensity ratio occurs is

$$S_{max}^{n_1-2} = \frac{n_1+1}{3}\left[S_p^{n_1-2} - \frac{\sigma_p^{n_1+1}}{B_1(n_1+1)\dot{\sigma}_u}\right] \qquad \text{(A7)}$$

The maximum strength at the beginning of unloading, S_{pmax}, that can begin in Region I and increase to Region II without crossing is, therefore, that value of S_p for which $\sigma_{max}/S_{max} = r$. This is found directly by solving Equations A6 and A7 for S_p and assigning that value to S_{pmax}

$$S_{pmax}^{n_1-2} = \frac{\sigma_p^{n_1+1}}{B_1(n_1+1)\dot{\sigma}_u} + \frac{3}{n_1+1}\left[\frac{B_1(n_1-2)\dot{\sigma}_u}{r^{n_1+1}}\right]^{(n_1-2)/3} \quad \text{(A8)}$$

Thus the strength of a flaw just avoiding Region II growth during unloading, S_{pmax}, can be determined

for this special case. Furthermore, the minimum strength after proof testing, S_{2min}, is determined by simply applying Region I mechanics once S_{pmax} is known

$$S_{2min}^{n_1-2} = S_{pmax}^{n_1-2} - \frac{\sigma_p^{n_1+1}}{B_1(n_1+1)\dot{\sigma}_u} \qquad \text{(A9)}$$

Combining Equation A8 and A9, the minimum post-proof strength for Scenario 2 of the case for Region I growth at the beginning of unloading is

$$S_{2min}^{n_1-2} = \sigma_p^{n_1-2}\frac{3}{n_1+1}\left[\frac{B_1(n_1-2)\dot{\sigma}_u}{\sigma_p^3\ r^{n_1+1}}\right]^{(n_1-2)/3} \quad \text{(A10)}$$

Although it is possible to model these Case 3 scenarios, an experimental verification of the model is needed.

References
1. E. R. FULLER Jr, S. M. WEIDERHORN, J. E. RITTER Jr and P. B. OATES, *J. Mater. Sci.* **15** (1980) 2282.
2. G. S. GLAESEMANN and J. D. HELFINSTINE, in "Proceedings for Fiber Optics Reliability and Testing: Benign and Adverse Environments", SPIE Vol. 2074, edited by D. Paul and H. Yuce (SPIE, Boston, 1993) p. 95.
3. G. S. GLAESEMANN, in "Proceedings of Optical Network Engineering and Integrity", SPIE Vol. 2611, edited by H. Yuce, D. Paul, and R. A. Greenwell (SPIE, Boston, 1995), p. 38.
4. B. R LAWN, in "Fracture of Brittle Solids" 2nd Edn (Cambridge University Press, 1993).
5. TIA/EIA-455-76, Method For Measuring Dynamic Fatigue of Optical Fibres by Tesion, edited by H. Yuce (Telecommunications Industry Association, Arlington VA, 1993).
6. B. A. PROCTOR, I. WHITNEY, and J. W. JOHNSON, *Proc. R. Soc. Lond. A* **297** (1967) 534.
7. S. M. WEIDERHORN, in "Fracture Mechanics of Ceramics", Vol. 2, edited by R. C. Bradt, D. P. H. Hasselman and F. Lange (Plenum Press, New York, 1974) p. 613.
8. TIA/EIA-455-31C, Proof Testing Optical Fibers by Tension, edited by T. A. Hansion (Telecommunication Industry Association, Arlington VA, 1994).